LAB 4:Navigation with IMU and Magnetometer

Robotics: Sensing and Navigation

Ronan McNally

mcnally.ro@northeastern.edu

Abstract

This document contains the results and analysis from using an IMU and GPS to keep track of the motion and position of a vehicle as it drives through Boston. It includes correcting for hard and soft iron distortions on a magnetometer, applying rotation matrices to correct for sensor misorientation, and comparing the results of different sensor readings to demonstrate the ability to employ multiple sensors to obtain a more accurate sense of motion and position.

Introduction

Locating where one is can become complicated when the sensors used to determine location are prone to errors. For example, global position system (GPS) pucks can be prone to errors from atmospheric interference as well as signals being reflected off other surfaces near the receiver while an inertial measurement unit (IMU) magnetometer (which relies on the magnetic field of the Earth to determine direction similar to a compass) can be prone to interference via hard and soft iron distortions. Hard iron distortions occur when an additional magnetic field is present and soft iron distortions are the result of nearby metal which can interfere with the detection of the magnetic field of the Earth (such as copper and nickel). Correcting for these errors both by analyzing and correcting for their sources as well as combining sensors can enable one to better locate oneself. Such is the purpose of this lab.

Procedure

Before collecting any data, the GPS and IMU were mounted to the vehicle used to collect data. The GPS was attached to the roof of the car while the IMU was placed inside the vehicle. Effort was taken to ensure the x-axis of the IMU aligned with the front of the car. The IMU was leveled using a level app on an iPhone. The IMU was fixed in place with the use of tape.
Upon securing the sensors in the car, the first trial was performed. In this trial, the vehicle was driven in a circular motion around the Ruggles rotary five times. The recording began, the car was started, the car stayed in place for ten seconds, then it began driving in five loops. At the end of this recording, the car was not turned off.
The next trial performed was that of a drive through Boston with multiple turns that looped back to the same location. The recording began, the car stayed in place for ten seconds, and then began driving its route. Occasional dead-end turns forced the vehicle to turn around. Upon arriving back at the same location, the recording was stopped. This data was then shared with each passenger within the car.

Results

Using the data from the circular driving pattern, the hard and soft iron distortions were corrected for. The original circular driving pattern data was elliptical and not centered at zero. These are the results of the soft and hard iron distortions respectively. **(1)** The ellipse not being centered at zero is indicative of a hard iron distortion from an external magnetic field interference (potentially as a result of being in proximity to the Ruggles train station), and the elliptical shape of the curve is indicative of soft iron distortions caused by metal (such as the car frame) surrounding the IMU. By using the MATLAB function fit_ellipse, values for the degrees of tilt, center points, and short and long axis lengths of the ellipse could be derived. First, the hard iron distortion effects could be removed by subtracting the center coordinate points of the ellipse from the x- and y-data. This translates the ellipse to the origin. Then the angle of tilt could be used to rotate the data via a rotation matrix. This makes the ellipse horizontal. From here, the data can be fit to a circle by multiplying the x-values (as the rotation makes this the only axis affected by soft iron distortions) by the ratio between the short-axis and long-axis of the ellipse. The results of this calibration can be seen in Figure 1 on the next page.

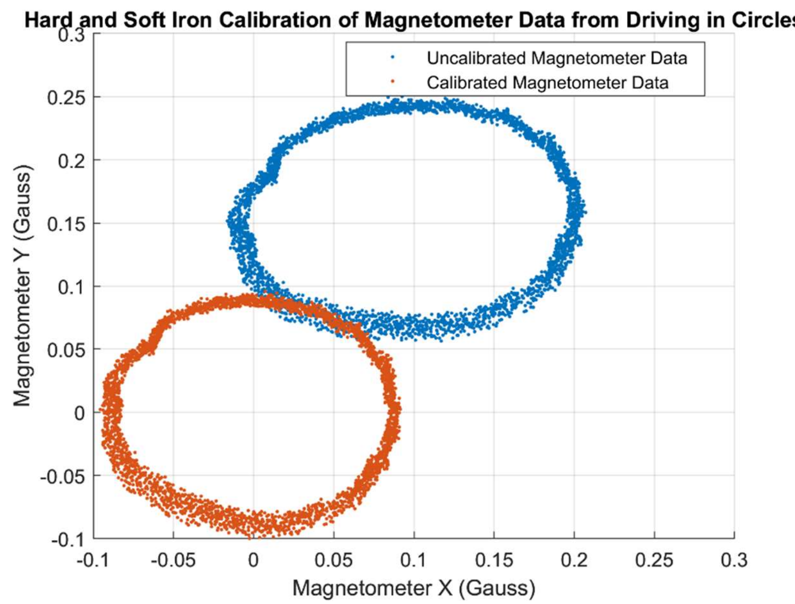

Figure 1: Circular Driving Magnetometer Data Before and After Hard and Soft Iron Distortion Corrections.

A slight elliptical shape is still present in the calibrated curve, but this can be attributed to imperfect driving. The values of calibration found here were then used to correct the Boston tour data.

Using the calibrated magnetometer data, a magnetometer yaw could be calculated using the relationship $yaw_{mag} = atan\left(\frac{-Mag_y}{Mag_x}\right)$. The function atan2 was used in MATLAB to have the function account for the entire cartesian interval. This relationship was used to find yaw values for both the raw and calibrated magnetometer data. A comparison of the two results can be seen in Figure 2 below.

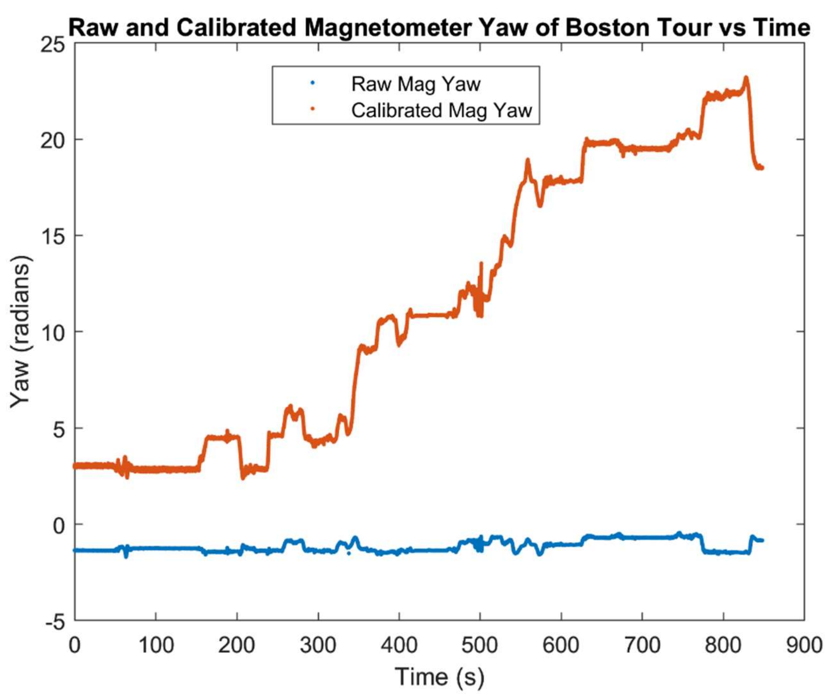

Figure 2: The Magnetometer Yaw Estimates Before and After Hard and Soft Iron Distortion Corrections.

Yaw values, or headings, were also found for the gyroscope sensor by integrating its recorded yaw rate with respect to time. **(2)** A low pass filter was then applied to the magnetometer yaw estimate and a high pass filter to the gyroscope yaw estimate using the lowpass and highpass functions of MATLAB respectively. The former had an fpass value was .001 and the latter had an fpass value of 17. The frequency of the signal for both was 40 Hz. Combining the results of these filters resulted in a complimentary filter effect. The result of calculating yaw from the magnetometer, the gyroscope, the combined filtering of the two, and the recorded yaw values from the VectorNav can all be seen in Figure 3 below.

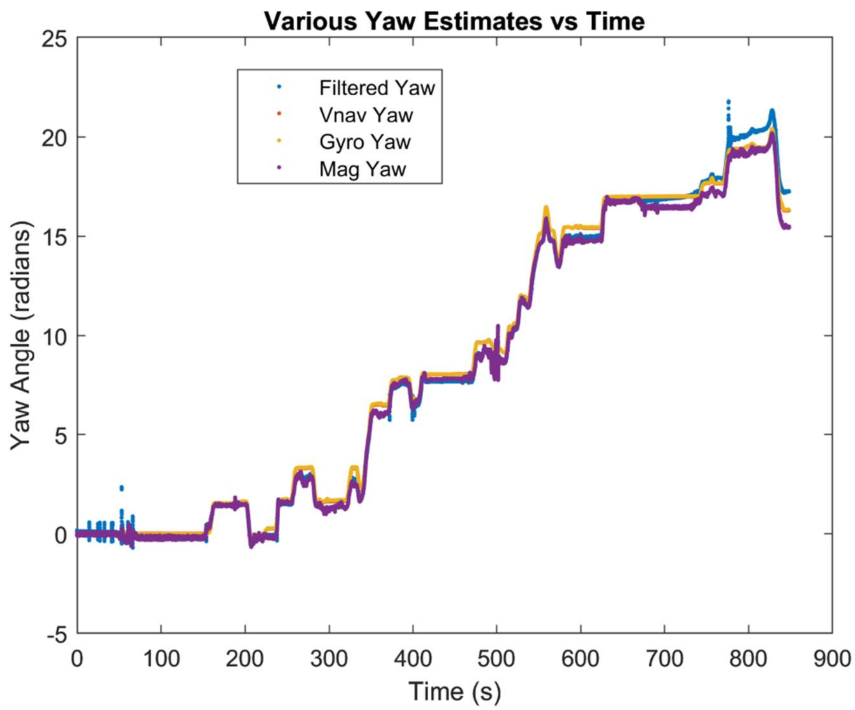

Figure 3: Yaw Estimates of the Gyroscope, Magnetometer, Complementary Filtered between the Gyroscope and Magnetometer, and the VectorNav.

From Figure 3 it can be seen that the yaw estimate derived from the magnetometer data and the yaw estimate derived from the gyroscope data are similar, following roughly the same shape. One difference between the two is that the magnetometer appears to have more noise with a rougher curve and trends lower than the gyroscopic yaw. A potential cause for this latter error could be magnetic drift. While difficult to see, the VectorNav yaw closely tracks with the gyroscopic yaw. It appears smoother better aligned with the other yaw estimates than the complimentary filter estimates from sensor fusion. **(3)** Of the estimates within Figure 3, I would most trust that of the gyroscope or the VectorNav as the two estimates agree closely and the magnetometer has vulnerability to distortions still potentially affects its accuracy and this will propagate into the combined filter between the gyroscope and the magnetometer. Estimates for the forward velocity of the car can be derived from the x-acceleration recorded by the IMU and from the GPS' position data. First, the acceleration was integrated with respect to time to find a velocity estimate from the IMU. However, this results in an unrealistic velocity which continuously increases to a value impossible for the vehicle used to collect data. **(4)** This can be attributed to drift within the accelerometer in which the propagation of small errors from a gradual bias in the readings of the accelerometer result in an error that propagates and magnifies when integrating to find velocity. To correct for these biases, the average value of periods in which zero acceleration was expected, but a non-zero average was present due to drift, were subtracted from the acceleration data incrementally. The first instance of drift was subtracted from all the date and each following instance of drift had its bias subtracted only from that instance within the data to the end of the data. At the end of this process is a calibrated acceleration that could then be re-integrated to find an improved velocity estimate. This source of error seamed to dominate over any present due to slight misalignment in the sensor. The difference between the initial and corrected estimates can be seen in Figure 4 below.

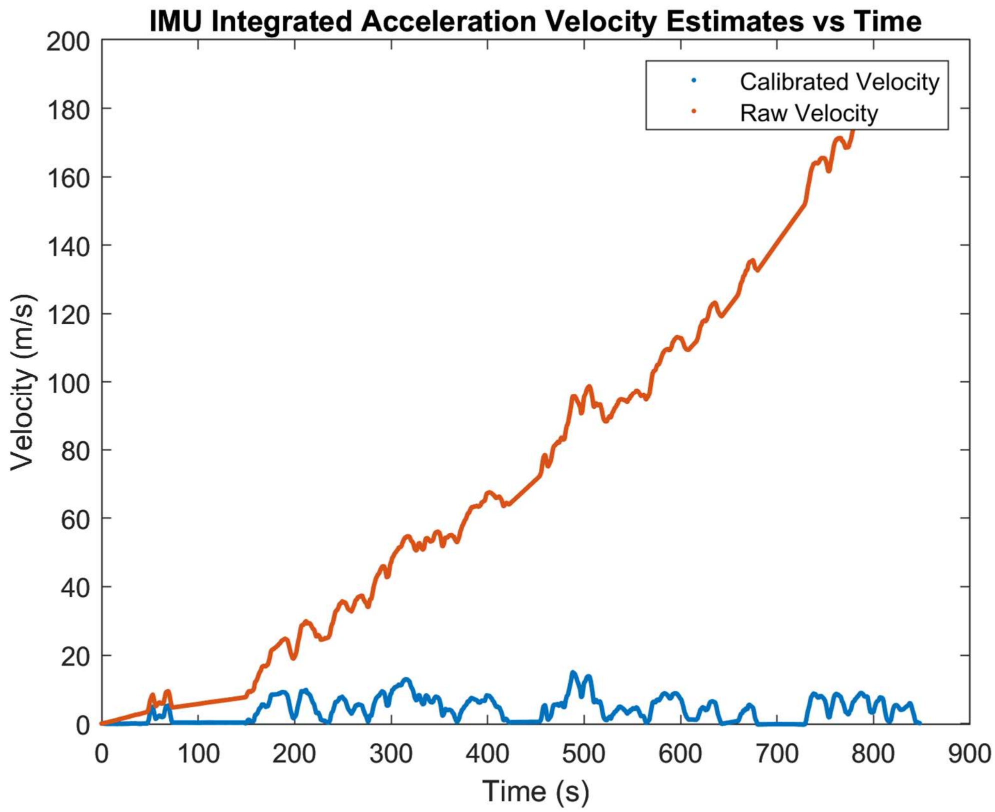

Figure 4: Velocity Estimates from Integrating IMU Forward Acceleration with Time Before and After Correcting for Accelerometer Drift.

From here an estimate for velocity could be found from the GPS position data. By using the Easting and Northing positions from the GPS and finding the distance between them using a rewriting of the Pythagorean theorem and then deriving with respect to time, a velocity estimate could be found. A comparison between the calibrated velocity estimate from acceleration and the GPS velocity estimate can be seen in Figure 5 on the next page.

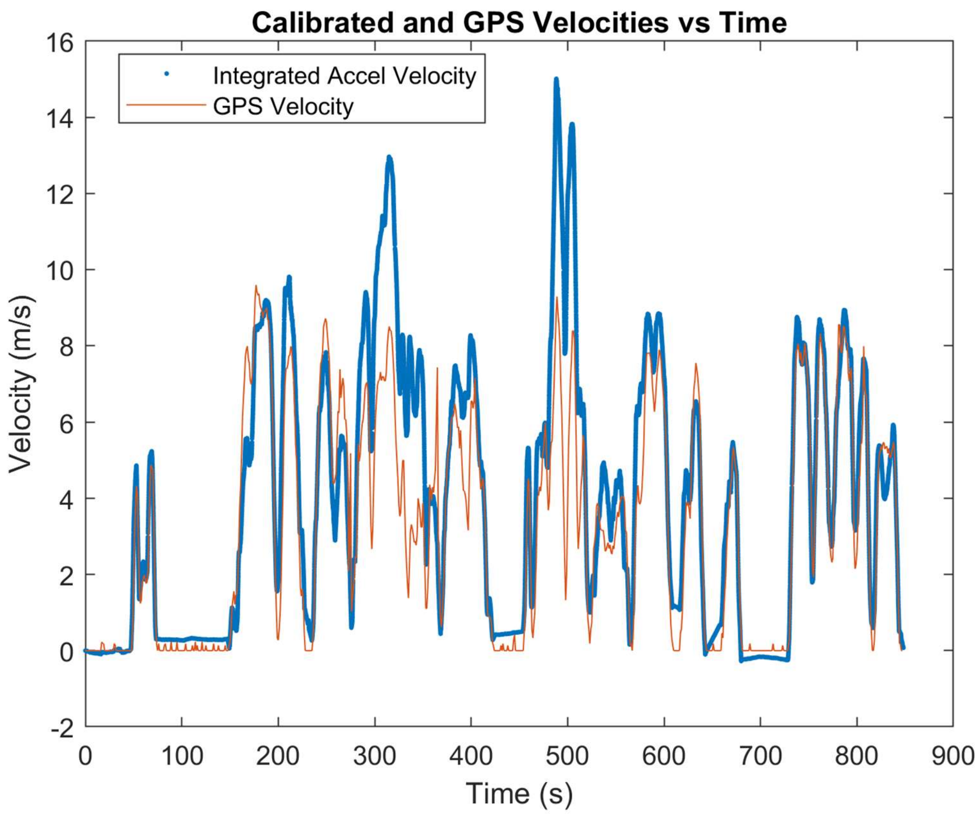

Figure 5: The Accelerometer Derived Velocity Calibrated for Drift Compared to the GPS Derived Velocity Over Time.

(5) As can be seen in Figure 5, there is still a slight misalignment between the magnetometer estimate and the GPS estimate. This can be attributed to slight misalignments in the IMU position resulting in a propagation of error.

Dead reckoning via the IMU could then be performed following these velocity estimations. By integrating the velocity obtained from the forward acceleration, distance traveled with respect to time could be found. Comparing this with the distance traveled calculated using the GPS data yield Figure 6 seen on the next page.

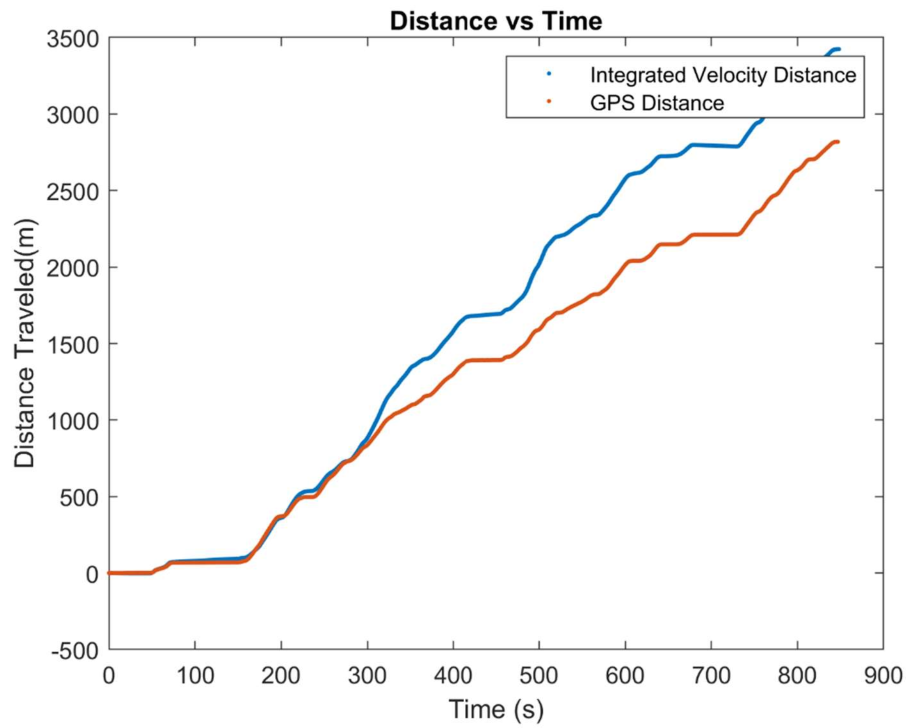

Figure 6: Comparison between Distances Traveled Derived from the Accelerometer and GPS Puck.

Once again, the slight misalignment in the IMU results in a propagated error when integrating the data. From here, using a simplified model of the equations of motion shown below,

$$\ddot{x}_{obs} = \ddot{X} - \omega\dot{Y} - \omega^2 x_c \quad (1)$$

$$\ddot{y}_{obs} = \ddot{Y} - \omega\dot{X} - \dot{\omega} x_c \quad (2)$$

where x_{obs} and y_{obs} are the observed x- and y- axis positions sensed by the IMU, X and Y are the x- and y-positions of the center of mass, x_c is the offset of the IMU from the center of mass, and ω is the yaw rate. Assuming the car is not sliding ($\dot{Y} = 0$) and the IMU is placed at the center of mass ($x_c = 0$), a calculation for the acceleration in the y-direction (as a result of the Coriolis effect) could be found using the equation $\ddot{y}_{calculated} = \omega\dot{X}$. Comparing the calculated y-acceleration with the observed y-acceleration of the IMU yields Figure 7 on the next page.

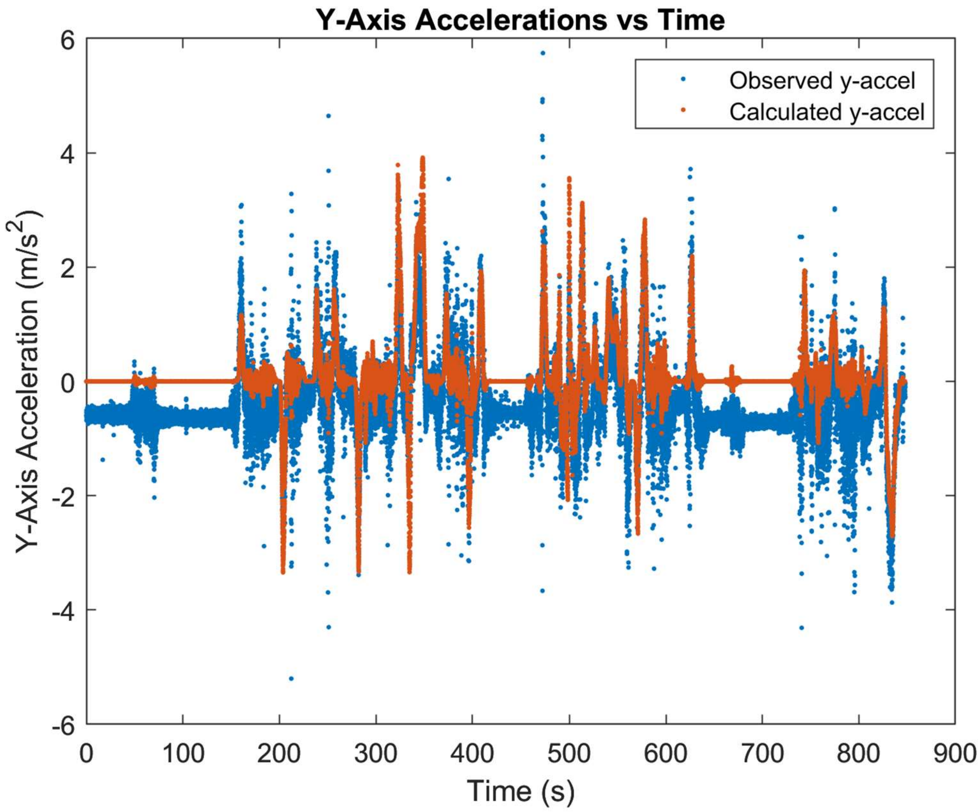

Figure 7: Derived Y-Acceleration and Y-Acceleration Observed by Accelerometer Over Time.

(6) As seen in Figure 7, these trends initially appear to match in shape but are shifted from one another. This can be attributed to the slight misalignment of the IMU resulting in the z-acceleration "bleeding" into the y. Applying a rotation matrix about x-axis to the acceleration data can correct this. The results of this rotation can be seen in Figure 8 on the next page.

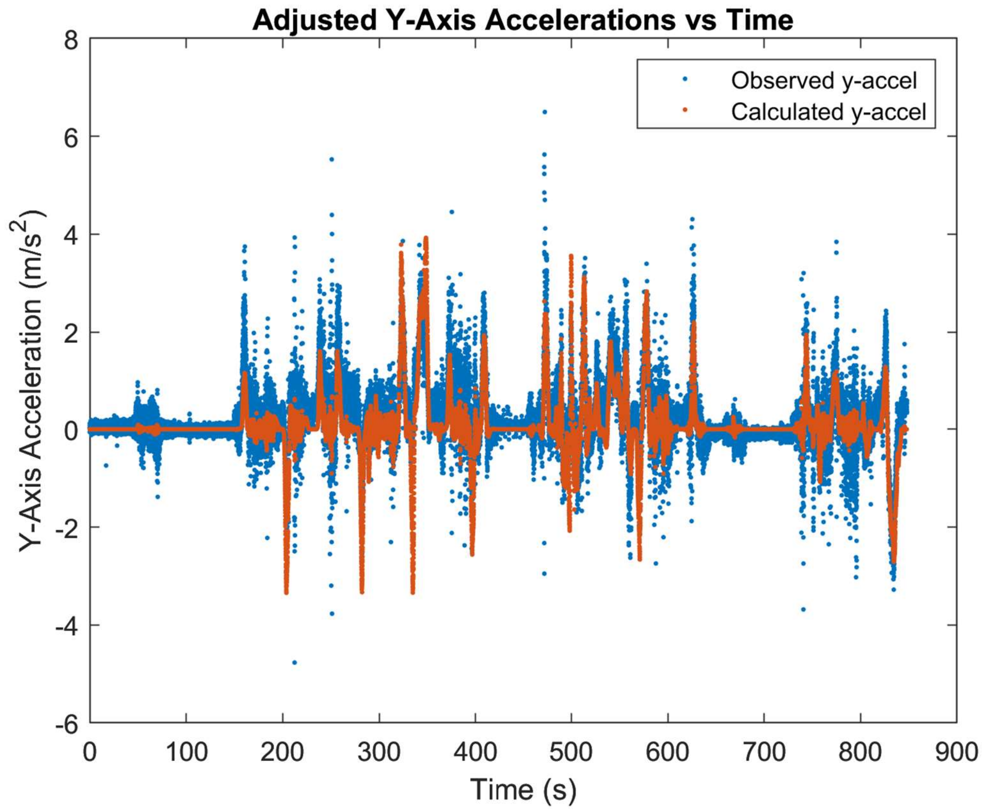

Figure 8: Calibrated Derived Y-Acceleration Compared to Y-Acceleration Observed by IMU Over Time.

As Figure 8 shows, the calculated and observed y-accelerations appear to follow the same pattern of rise and fall. While the observed y-acceleration from the IMU shows higher amplitude spikes, this can be attributed to its lower precision (indicated by its greater spread about 0) and misalignment in the IMU within the recorded acceleration data.

(7) From here, the estimated trajectory of the sensors along the Boston tour route could be found via the GPS data as well as by separating the forward velocity into Easting and Northing components using the sine and cosine of the yaw angle and then integrating to find position data. Scaling the calculated position data by a factor of 50 to match in size with the GPS position data results in Figure 9 seen on the next page.

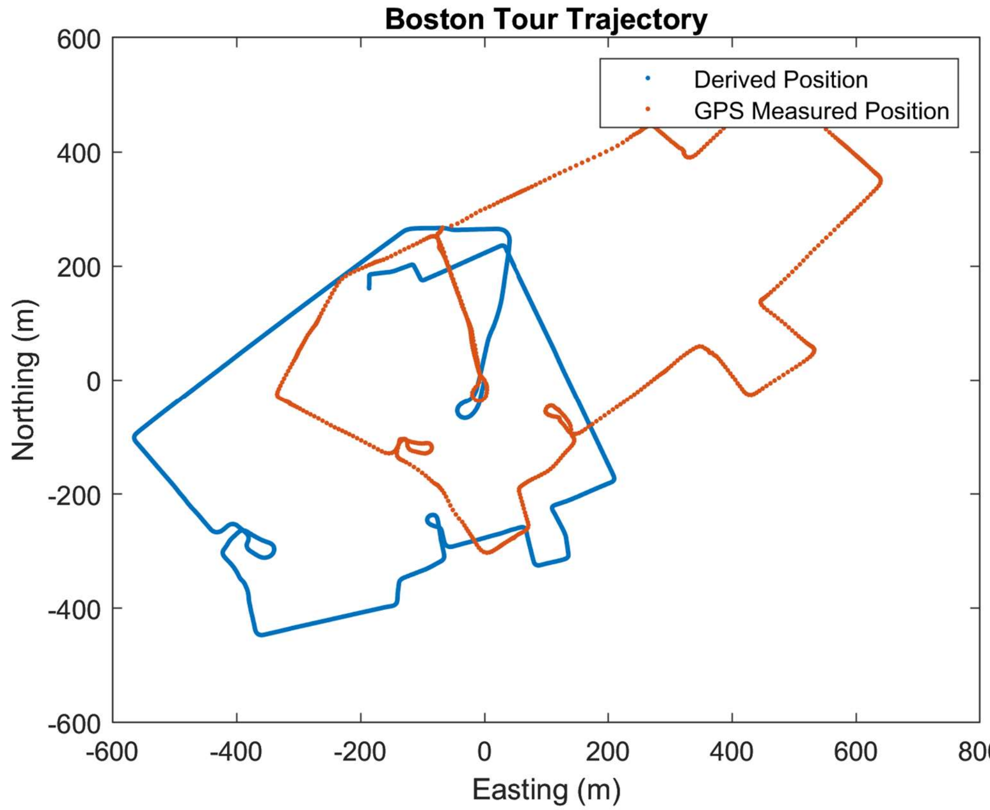

Figure 9: Results of Dead Reckoning Boston Tour Trajectory from GPS Data and by Deriving Position from Yaw and Forward Velocity.

As can be seen in Figure 9, the GPS data is more accurate while the calculated trajectory appears to consistently bend throughout, resulting in a trajectory shape that almost appear to have been twisted. This can be attributed to IMU misalignment that has not been corrected resulting in the derived yaw used in the calculation being slightly erroneous and that error propagating in the integration. **(8)** Given the specifications of the VectorNav and assuming this is with respect to driving in a vehicle, I would assume it could remain accurate for at a few minutes if it could rely on other sensors. The gyroscope of the IMU for instance was very close to the GPS data for yaw estimates after all. The GPS and IMU estimates shown in Figure 9 though stop matching closely within the first few seconds of beginning the drive. The stated performance of dead reckoning did not match the actual measurements well. This can likely be attributed to uncorrected remaining misalignment in the IMU. The integration of the acceleration results in minor misalignments of the IMU propagating and magnifying within the derived position data.

Conclusion

By correcting for the hard and soft iron distortions in the circular driving data and applying these corrections to the driving data, the calibrated magnetometer data, gyroscope angle rate data, linear acceleration data, recorded angle data, and GPS data could be used to derive various estimates for yaw, forward velocity, distance traveled, and position. Comparing these values and how they are alike or different gives a sense of how multiple sensors can be compared to refine the estimate of where one is. However, one point to note is that the sensor fusion between the magnetometer and gyroscope estimates of yaw did not result in a more refined estimate for yaw. This could be attributed to lingering magnetic drift. This is most evident in the estimate for yaw angle in Figure 3 and Figure 5 in which the estimated yaws and forward velocities line up. This is enabled by correcting for, in addition to hard and soft iron distortions, accelerometer drift and IMU position. Sources of error that couldn’t be corrected for are where assumptions about the nature of data collection don’t hold up: assuming that motion only occurs in a 2D plane when driving did occur at different elevations and that the IMU was centered at the center of mass of the vehicle.